A Journal of the German Chemical Society

Angewandte Chemie

GDCh

International Edition

www.angewandte.org

2019–58/29

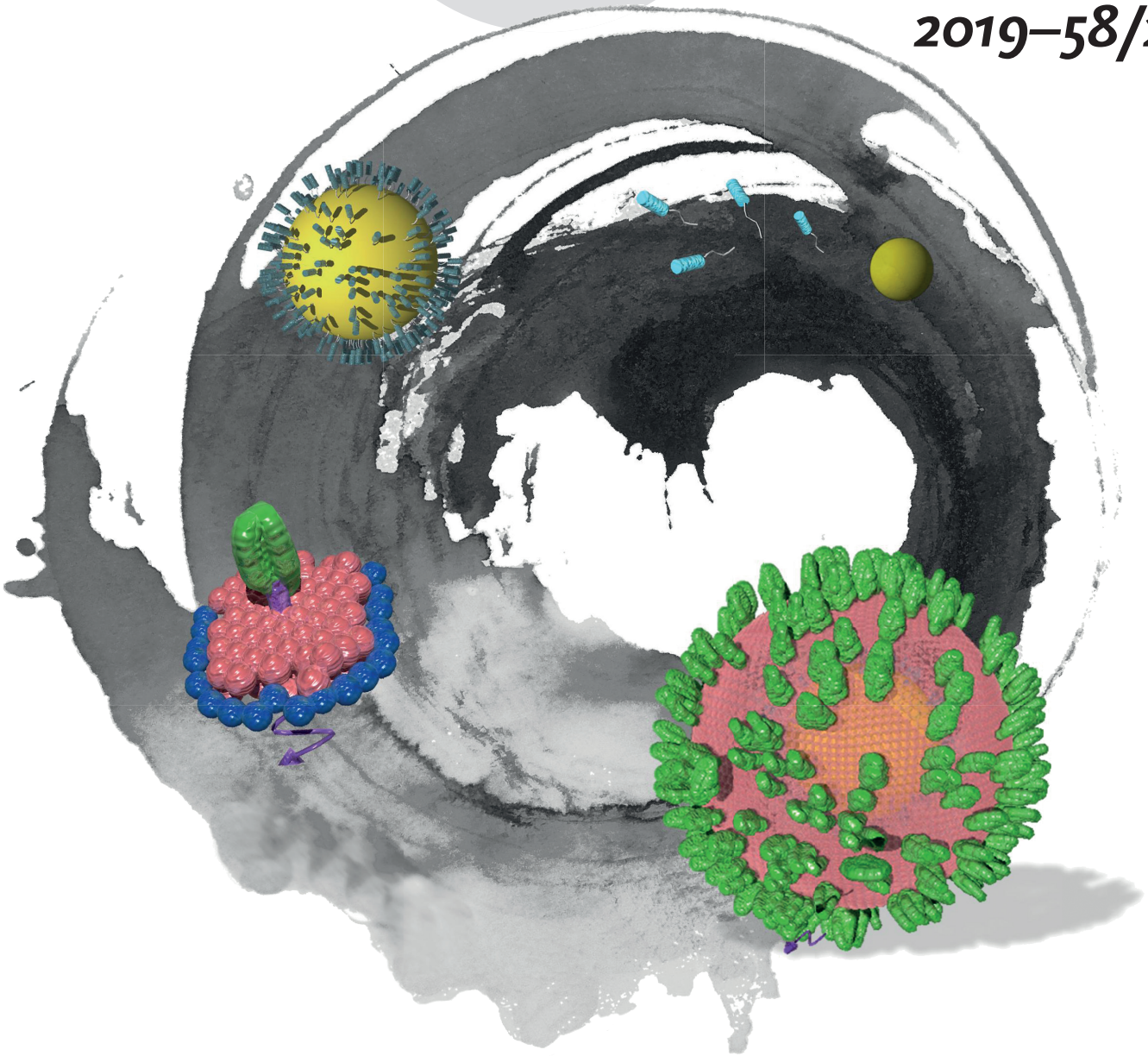

Presentation of membrane proteins ...

… to host immune systems in a conformation-specific manner is a major challenge in vaccine or antibody development. In their Communication on page 9866 ff., J. Guo, J. J. Chou, et al. developed a method to address this challenge. They used a functionalized nanoparticle as a substrate to guide the formation of proteoliposome that can unidirectionally present many copies of membrane proteins.

WILEY-VCH

Nanoparticles

International Edition: DOI: 10.1002/anie.201903093
German Edition: DOI: 10.1002/ange.201903093

Unidirectional Presentation of Membrane Proteins in Nanoparticle-Supported Liposomes

Wen Chen, Yongfei Cai, Qingshan Fu, Bing Chen, Junling Guo, and James J. Chou**

Abstract: *Presentation of membrane proteins to host immune systems has been a challenging problem owing to complexity arising from the poor in vivo stability of the membrane-mimetic media often used for solubilizing the membrane proteins. The use of functionalized, biocompatible nanoparticles as substrates is shown to guide the formation of proteoliposomes, which can present many copies of membrane proteins in a unidirectional manner. The approach was demonstrated to present the membrane-proximal region of the HIV-1 envelope glycoprotein. These nanoparticle-supported liposomes are broadly applicable as membrane antigen vehicles for inducing host immune responses.*

The large majority of antibodies currently being developed for therapeutic use target membrane-anchored or integral membrane proteins. Presenting these proteins to immune systems to induce antibodies is however a difficult problem, in particular for those whose structural integrity can only be preserved on the membrane. Several approaches have been developed to address this problem. Liposomes are often used as membrane protein carriers for inducing immune responses.[1] During liposome formation, however, the protein orientation is random. The unstable nature of liposome, that is, its tendency to fuse with other cellular vesicles, could be another source of risk in its application. Greater stability in serum could be achieved using interbilayer-crosslinked multilamellar vesicle (ICMV)-coated particles,[2] but the technique has not been demonstrated to incorporate transmembrane proteins. Lipid nanodisc is another popular medium for membrane proteins,[3] and has been used previously in phage display.[4] But, nanodisc samples are generally difficult to make in large quantities. Moreover, regular nanodiscs usually can only contain 1–2 copies of protein owing to its small size (10–15 nm in diameter),[5] and are thus not ideal for inducing strong immunogenic responses in vivo. It is also possible to use mammalian cells to produce virus-like particles (VLP) incorporating membrane proteins on the VLP membrane.[6] The success of this approach, however, depends on the efficiency of protein incorporation into VLP, which needs laborious optimization for each target and often cannot be controlled manually.

We sought to use nanoparticles as substrates to guide proteoliposome assembly. By modifying nanoparticles with functional moieties that specifically recruit affinity-tagged membrane proteins in bicelles, we could form proteoliposome around the nanoparticle where the proteins are presented in a unidirectional manner. We have demonstrated this approach, named supported proteoliposome for antigen directed display (SPLANDID), for a membrane fragment of the HIV-1 envelope glycoprotein (Env) encompassing the transmembrane (TM) domain and the membrane-proximal external region (MPER).

The design concept, illustrated in Figure 1 a–d, is to specifically recruit membrane proteins solubilized in lipid/detergent bicelles (which closely mimic a lipid bilayer) to the surface of a globular shaped nanoparticle, also referred to as the substrate. As detergent is removed, the protein-containing bicelles will grow on the substrate surface to form proteoliposomes. Nanoparticles can take on various forms and compositions. For biological or medical applications, it is important that the particles are biocompatible with no major toxic or immunogenic risk to biological organisms. We experimented with two different types of nanoparticles (Figure 1 a). One is natural polyphenol-stabilized gold nanoparticle (AuNP), which is solid and can be fabricated to various sizes ranging from 3 to 50 nm by exploiting the coordination and stabilization of gold ions with polyphenol moieties.[7] AuNPs are biocompatible and have been approved by FDA as generally recognized as safe (GRAS) and for drug use.[8] Polyphenol moieties can be further functionalized via their hydroxy groups and active carbon sites.[9] Another form of nanoparticle is the hollow DNA buckyball assembled by DNA origami.[10] DNAs are generally non-immunogenic.[11] A variety of modifications can be incorporated into DNA during synthesis for functionalization.

In our assembly method, membrane proteins are purified and solubilized in bicelles composed of 1,2-dimyristoyl-sn-glycero-3-phosphocholine (DMPC) and 1,2-dihexanoyl-sn-glycero-3-phosphocholine (DH_6PC) (Supporting Information, Experimental Procedures; Figure 1 b). An affinity tag is placed at the cytoplasmic end of the protein for directing the protein to the nanoparticles. In the current study, this affinity tag is a polyhistidine tag (His_6-tag), and the functional

[*] Dr. W. Chen, Dr. Q. Fu, Prof. J. J. Chou
Department of Biological Chemistry and Molecular Pharmacology, Harvard Medical School
250 Longwood Avenue, Boston, MA 02115 (USA)
E-mail: james_chou@hms.harvard.edu
Dr. Y. Cai, Prof. B. Chen
Division of Molecular Medicine, Boston Children's Hospital, Department of Pediatrics, Harvard Medical School
3 Blackfan Street, Boston, MA 02115 (USA)
Prof. J. Guo
Department of Biomass Science and Engineering, Sichuan University
24 South Section Yihuan Road, Chengdu, Sichuan 610065 (China)
E-mail: junling.guo@scu.edu.cn
Supporting information and the ORCID identification number(s) for the author(s) of this article can be found under: https://doi.org/10.1002/anie.201903093.

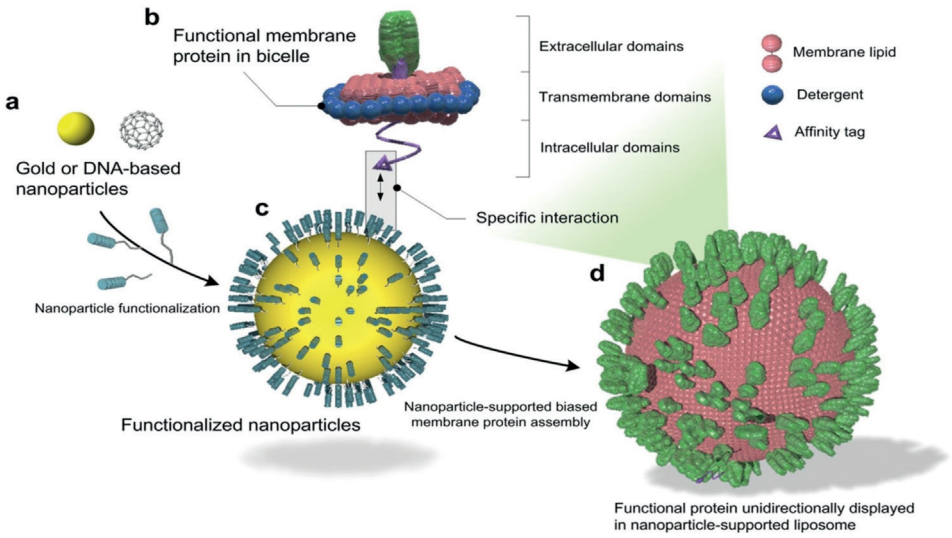

Figure 1. Illustration of nanoparticle-supported proteoliposome for unidirectional presentation of membrane proteins. a) The solid nanoparticle (for example, polyphenol-stabilized gold nanoparticle) and the hollow DNA buckyball can both be used as core substrates for liposome formation. b) Membrane proteins with cytoplasmic affinity tag are reconstituted in bicelles that mimic a lipid bilayer. c) Functional moieties for interacting with the protein affinity tag are covalently linked to the nanoparticles. d) High copy numbers of membrane proteins are presented in a unidirectional manner in a nanoparticle-supported liposome.

moieties on the nanoparticles are Ni-NTAs (Figure 1c). Only bicelles containing the membrane protein of interest will specifically "glue" to the nanoparticle surface via (Ni-NTA)–(His_6-tag) interaction, and since the His_6-tag is on the cytoplasmic side of the protein, the protein–bicelle complex will be glued in a unidirectional manner. As DH_6PC is removed, the bicelles will merge and form proteoliposome encapsulating the nanoparticle (Figure 1d).

AuNPs were synthesized by mixing the gold precursor, gold(III) chloride ($HAuCl_4$), and tannic acid (TA) solution as described previously (Supporting Information, Experimental Procedures).[7a] The phenolic hydroxy groups (−OH) of TA can coordinate with the Au^{3+} ions and act as reducing agent and surfactant to stabilize the synthesized AuNPs (Supporting Information, Figure S1a). The size of the AuNPs can be precisely controlled by the ratio of gold precursor to TA and their stirring speed of the reaction. We first prepared AuNPs with average diameter of about 47 nm, as shown by transmission electron microscopy (TEM) (Figure 2a) and dynamic light scattering (DLS) (Supporting Information, Figure S2a). The AuNPs were then functionalized with lysine–NTA (Supporting Information, Experimental Procedures) by conjugating the amine groups of lysine–NTA and the nucleophilic carbons of the phenolic aromatic rings via glutaraldehyde (Figure 2a; Supporting Information, Figure S1b). The NTA-AuNPs further coordinated Ni^{II} upon the addition of Ni^{2+} ions into the NTA-AuNPs nanoparticle suspension. The surface charges of AuNPs, evaluated as the zeta potential (ξ), were monitored during the functionalization process. As shown in the Supporting Information, Figure S2b, the polyphenol-stabilized AuNPs are negatively charged ($\xi = -52$ mV) owing to deprotonation of the hydroxy groups. The ξ increased to −36 mV after conjugation with lysine–NTA and increased further to −20.1 mV after addition of Ni^{2+}, as a result of modification of polyphenol groups and coordination with positively charged Ni^{2+}, respectively. Finally, to examine the ability of the Ni-NTA functionalized AuNPs (Ni-NTA-AuNPs) to specifically interact with His_6-tag, we recorded 1D ^1H NMR spectrum of the Foldon protein containing C-terminal His_6-tag (Foldon-His_6) before and after mixing with the Ni-NTA-AuNPs (see the Supporting Information, Experimental Procedures). The Foldon NMR signals were essentially ablated

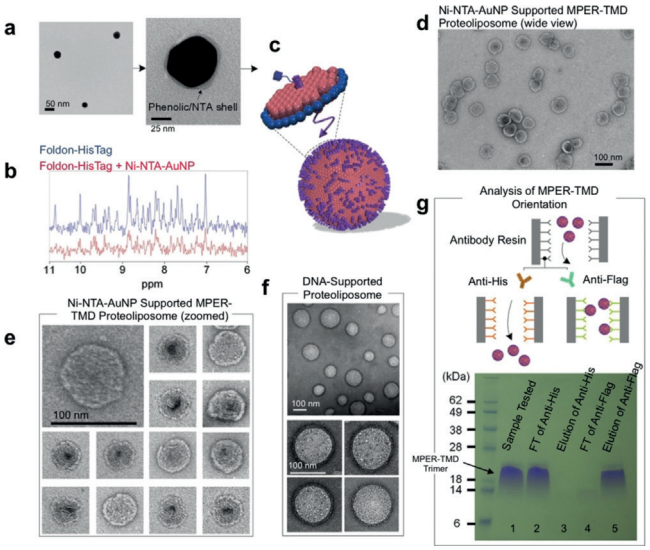

Figure 2. Nanoparticle-supported proteoliposome formation using bicelle-reconstituted MPER-TMD. a) TEM images of gold-polyphenol nanoparticles (AuNPs) functionalized with NTA (NTA-AuNP). b) ^1H NMR spectra the Foldon protein with C-terminal His_6-tag in the absence and presence of Ni-NTA-AuNPs. Blue: 450 μL of 30 μM Foldon-His_6; Red: 450 μL of 30 μM Foldon-His_6 mixed with 100 μL of Ni-NTA-AuNP ($OD_{530} = 0.1$; the volume of the mixture adjusted to 450 μL before NMR measurement). c) Illustration of unidirectional coating of bicelle-reconstituted MPER-TMD onto Ni-NTA-AuNP. d) Negative staining EM (nsEM) image (wide view) of Ni-NTA-AuNP supported MPER-TMD proteoliposome (see text). e) nsEM images of the Ni-NTA-AuNP-supported MPER-TMD proteoliposomes at two magnifications. f) nsEM images of DNA buckyball-supported MPER-TMD proteoliposomes at two magnifications. g) Analysis of FLAG-MPER-TMD-His_6 orientation in Ni-NTA-AuNP-supported liposomes by antibody resin pull-down and SDS-PAGE. Lane 1: Ni-NTA-AuNP-supported MPER-TMD liposome; Lane 2: flow-through from anti-His_6 resin after 30 minutes incubation; Lane 3: elution from anti-His_6 resin; Lane 4: flow-through from anti-FLAG resin after 30 minutes incubation; Lane 5: elution from anti-FLAG resin.

upon the addition of Ni-NTA-AuNPs (Figure 2b), indicating strong binding of Foldon-His_6 to the nanoparticles that caused NMR signals to decay rapidly.

Having generated Ni-NTA-AuNPs, we next tested the above scheme of proteoliposome formation using a fragment of HIV-1 Env that contains the membrane-proximal external region (MPER) and the transmembrane domain (TMD). This fragment (residues 660–710) is derived from a clade D HIV-1 isolate 92UG024.2 (designated MPER-TMD).[12] The MPER is one of the most conserved regions of HIV-1 Env and bears epitopes of broadly neutralizing antibodies from infected individuals.[13] Therefore, methods for presenting the MPER to human immune system are of strong interest to HIV vaccine development.

We introduced a His_6-tag at the C-terminus of the MPER-TMD to interact with the Ni-NTA-AuNPs. The MPER-TMD was expressed, purified, and reconstituted in bicelles with $q = 0.5$ as described previously.[12,14] The Ni-NTA-AuNP solution ($OD_{530} = 0.1$) and the solution of bicelle-reconstituted MPER-TMD-His_6 (0.3 mM) were mixed at a volume ratio of 3:1 to allow coating of protein-containing bicelles onto the nanoparticle surface (Figure 2c). After complete removal of DH_6PC by dialysis, relatively uniformly sized liposomes were formed around the nanoparticles (Figure 2d,e). The diameter of the liposomes is 75 ± 5 nm, which is consistent with the predicted size of the complex, including the Ni-NTA-AuNP (ca. 50 nm), the lipid bilayer (ca. 6 nm × 2), and the space between Ni-NTA-AuNP and lipid envelope. To provide additional evidence that the formation of stable nanoparticle-supported liposome is due to specific interaction between Ni-NTA and His_6-tag, we performed a series of control experiments, namely forming liposomes 1) with empty bicelles in the absence of AuNPs (Supporting Information, Figure S3a), 2) by mixing Ni-NTA-AuNPs with empty bicelles (Supporting Information, Figure S3b), and 3) by mixing non-functionalized AuNPs with bicelle-reconstituted MPER-TMD (Supporting Information, Figure S3c). As shown by negative staining EM (nsEM), liposomes formed under these conditions were mostly broken and highly inhomogeneous, indicating that direct recruitment of bicelles onto the nanoparticles via the membrane protein affinity tag is crucial to achieving homogeneous proteoliposome assemblies.

To achieve the highest proteoliposome assembly efficiency, different ratios of Ni-NTA-AuNP to MPER-TMD-His_6 were tested. When the volume ratio between the solution of Ni-NTA-AuNP ($OD_{530} = 0.1$) and the solution of bicelle-reconstituted MPER-TMD-His_6 (0.3 mM) was set at 1:1, in addition to the expected liposome size (ca. 75 nm), much smaller liposomes (< 20 nm) were observed (Supporting Information, Figure S3d), likely formed with excessive MPER-TMD-His_6 and DMPC lipid without the support of Ni-NTA-AuNP. When the ratio was set to 3:1 and 6:1, the smaller liposomes mostly disappeared and very similar liposome populations were observed (Supporting Information, Figure S3e, S3f), suggesting that all protein-containing bicelles were recruited to Ni-NTA-AuNPs at the two ratios. Excessive Ni-NTA-AuNPs could not be observed owing to incompatibility with negative staining.

We next tested the use of hollow DNA nanoparticles to guide proteoliposome assembly. We used a previously designed DNA buckyball formed with three different DNA strands (long, medium, and short).[10] To functionalize the DNA buckyballs with NTA moieties, we used the TriNTA with modified primary amine,[15] which can be covalently linked to thiol-modified DNA via an amine-to-sulfhydryl crosslinker (Supporting Information, Figure S4a). As such, the long strand was synthesized with the dithiol group at the 3′ end, and TriNTA was covalently linked to the long strand via a bi-functional crosslinker, PEG2-SMCC (Supporting Information, Experimental Procedures). When charged with Ni^{2+}, the TriNTA has high binding affinity for the His_6-tag (20 ± 10 nM).[15] The TriNTA-linked DNA strand was purified and mixed with the other two strands to form DNA buckyballs with an average diameter of about 80 nm (Supporting Information, Figure S4b, S5). As in the AuNP application above, the bicelle-reconstituted MPER-TMD (with C-terminal His_6-tag) was mixed with the DNA buckyballs, and the ratio of MPER-TMD trimer to TriNTA (or long strand) was kept approximately at 1:1 to achieve about 60 MPER-TMD trimers per buckyball (there are 60 long strands in the assembly[10]). Upon removal of DH_6PC, spherical liposomes with diameter of 95 ± 15 nm were formed (Figure 2f; Supporting Information, Figure S6). We note that a fraction of liposomes are smaller than estimated size, probably because some DNA buckyballs were not completely assembled (thus smaller size) but could still catalyze liposome formation. More robust buckyball assembly can be achieved by using additional supportive DNA strands.[16]

To examine whether the MPER-TMD was unidirectionally presented on Ni-NTA-AuNP-supported liposomes, we introduced a FLAG-tag and a His_6-tag at the N- and C-termini of the MPER-TMD, respectively, and examined their relative accessibility to antibodies using an antibody resin pull-down assay. The Ni-NTA-AuNP-supported proteoliposomes containing the FLAG-MPER-TMD-His_6 were prepared using the same protocol as described above. Equal amounts of the assembled proteoliposomes were incubated with anti-FLAG and anti-His_6 resins separately. The flow-throughs from the resins were collected as readout of MPER-TMDs that do not bind the antibodies. Further, a 0.1 M glycine solution was used to elute the resin-bound fraction. The samples from flow-through and elution were analyzed by SDS-PAGE. For the anti-His_6 resin, 97.1% of MPER-TMDs were found in the flow-through (Figure 2g; Supporting Information, Figure S7; lanes 2, 3), whereas 94.8% of the MPER-TMDs were retained by the anti-FLAG resin (Figure 2g; Supporting Information, Figure S7; lanes 4, 5). The results indicate that the MPER-TMD was incorporated in the nanoparticle-supported liposomes in a unidirectional manner.

Finally, to test whether the nanoparticle-supported proteoliposomes are immunogenic, five guinea pigs were immunized with Ni-NTA-AuNP-supported MPER-TMD proteoliposome with Adju-Phos adjuvant. Animal sera from different time points (Figure 3a) were used to assess the ability of the vaccination regimen to elicit antibodies that can bind MPER-TMD reconstituted in regular liposome. The results from the

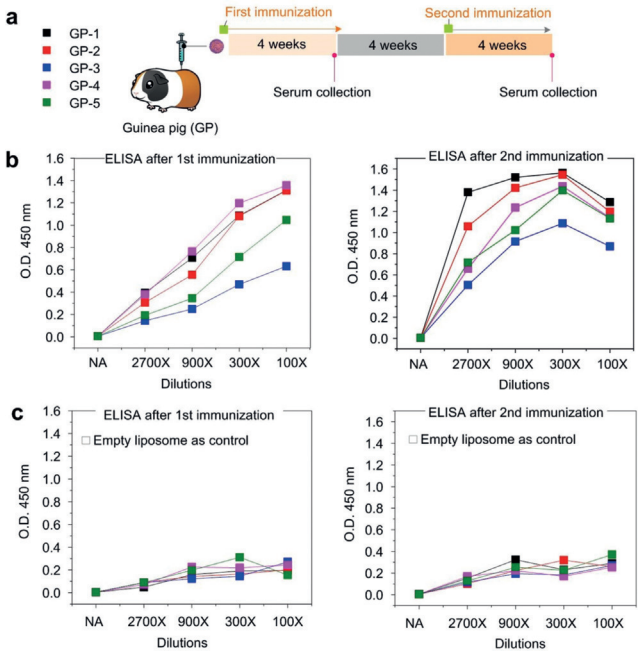

Figure 3. Immunogenicity of Ni-NTA-AuNP-supported MPER-TMD proteoliposomes. a) Immunization schedule of 5 guinea pigs. Serum samples were collected at weeks 4 and 12. b) ELISA analysis of serum for anti-MPER-TMD antibodies. ELISA plates were coated with MPER-TMD in regular liposomes. Sera were added in serial dilutions (2700, 900, 300, 100) and detected with a horseradish peroxidase (HRP)-conjugated rabbit anti-guinea pig secondary antibody for total IgG ELISAs. c) ELISA plate incubated with empty liposomes.

enzyme-linked immunosorbent assay (ELISA) show that all of the sera after the first vaccination already contained MPER-TMD binding antibodies, and that sera from the second immunization elicited antibodies that bind much stronger and more robust to MPER-TMD (Figure 3b). As a negative control, no binding to the empty liposome was observed (Figure 3c).

We have shown that nanoparticles with functionalized surface can serve as effective guide for the formation of proteoliposomes with unidirectional presentation of membrane proteins. Since the protein affinity tag drives uniform coating of bicelles, which are essentially solubilized membrane patches, around the nanoparticles, proteoliposome formation upon detergent removal is highly robust. Moreover, varying sizes of proteoliposomes are achievable for different applications, as the size of the nanoparticle substrate can be accurately controlled.

We believe the nanoparticle-supported liposomes can be effective vaccine carriers. First, potentially high copy number of membrane proteins can be incorporated. The unidirectional presentation further increases the amount of effective antigens for the immune system. Second, the AuNP used in the current study is highly biocompatible and inexpensive to produce. The presence of nickel inside the liposome may be a safety concern but its toxicity is expected to be greatly reduced when chelated by NTA.[17] Finally, the nanoparticle-supported liposome is structurally more stable than the regular liposomes owing to the nanoparticle-protein interaction, and such enhanced stability is important for application in vivo.

Previous attempts at presenting MPER in immunogens have not been successful in inducing neutralizing antibodies in vivo.[18] The failure could be due to the conformation nature of the epitopes or their limited accessibility on the membrane surface. Recent studies suggest lipid bilayer also accounts for the neutralizing potency of MPER-specific antibodies.[19] The reported method allowed unidirectional presentation of many MPER-TMD trimers on a single particle in a lipid bilayer environment. Indeed, the new immunogen elicited MPER-specific antibodies in the guinea pigs, though the neutralizing potential of these antibodies remains to be investigated.

In conclusion, the use of functionalized nanoparticles to guide proteoliposome formation offers many distinct advantages, including the improved efficiency and uniformity of liposome formation, the unidirectional presentation of transmembrane proteins, the preservation of membrane protein native structure, the greater control of protein incorporation number per liposome, and the greater stability of the nanoparticle-supported liposomes. While these advantages are particularly important for vaccine development, they are equally useful for developing therapeutic antibodies against membrane proteins such as GPCRs, transporters, and ion channels.

Acknowledgements

We thank Liqiang Pan for the insightful discussion. This work was supported by NIH grant AI127193 (to B.C. and J.J.C.), and GM116898 (to J.J.C.). J.G. is grateful to the China National Youth Talents Program and Double First Class University Plan of Sichuan University.

Conflict of interest

W.C., J.G., B.C., J.J.C. declare competing financial interests. A provisional patent was been filed on behalf of the Harvard Medical School.

Keywords: HIV-1 MPER · membrane antigen presentation · nanoparticles · proteoliposome formation · unidirectionality

How to cite: *Angew. Chem. Int. Ed.* **2019**, *58*, 9866–9870
Angew. Chem. **2019**, *131*, 9971–9975

[1] a) D. G. Russell, J. Alexander, *J. Immunol.* **1988**, *140*, 1274–1279; b) J. L. Rigaud, D. Levy, *Methods Enzymol.* **2003**, *372*, 65–86; c) L. K. Jespersen, A. Kuusinen, A. Orellana, K. Keinanen, J. Engberg, *Eur. J. Biochem.* **2000**, *267*, 1382–1389.
[2] a) J. J. Moon, H. Suh, A. Bershteyn, M. T. Stephan, H. Liu, B. Huang, M. Sohail, S. Luo, S. H. Um, H. Khant, J. T. Goodwin, J. Ramos, W. Chiu, D. J. Irvine, *Nat. Mater.* **2011**, *10*, 243–251; b) S. Pejawar-Gaddy, J. M. Kovacs, D. H. Barouch, B. Chen, D. J. Irvine, *Bioconjugate Chem.* **2014**, *25*, 1470–1478.
[3] N. R. Civjan, T. H. Bayburt, M. A. Schuler, S. G. Sligar, *Biotechniques* **2003**, *35*, 556–560, 562–563.

[4] a) M. Pavlidou, K. Hanel, L. Mockel, D. Willbold, *PloS one* **2013**, *8*, e72272; b) P. K. Dominik, A. A. Kossiakoff, *Methods Enzymol.* **2015**, *557*, 219 – 245; c) P. K. Dominik, M. T. Borowska, O. Dalmas, S. S. Kim, E. Perozo, R. J. Keenan, A. A. Kossiakoff, *Structure* **2016**, *24*, 300 – 309.
[5] a) T. H. Bayburt, S. G. Sligar, *FEBS Lett.* **2010**, *584*, 1721 – 1727; b) M. A. Schuler, I. G. Denisov, S. G. Sligar, *Methods Mol. Biol.* **2013**, *974*, 415 – 433.
[6] a) E. V. Grgacic, D. A. Anderson, *Methods* **2006**, *40*, 60 – 65; b) N. Kushnir, S. J. Streatfield, V. Yusibov, *Vaccine* **2012**, *31*, 58 – 83; c) L. H. Lua, N. K. Connors, F. Sainsbury, Y. P. Chuan, N. Wibowo, A. P. Middelberg, *Biotechnol. Bioeng.* **2014**, *111*, 425 – 440.
[7] a) J. Guo, H. Wu, X. Liao, B. Shi, J. Phys. Chem. C. **2011**, 115, 23688 – 23694; b) J. Guo, Y. Ping, H. Ejima, K. Alt, M. Meissner, J. J. Richardson, Y. Yan, K. Peter, D. von Elverfeldt, C. E. Hagemeyer, *Angew. Chem. Int. Ed.* **2014**, *53*, 5546 – 5551; *Angew. Chem.* **2014**, *126*, 5652 – 5657.
[8] a) H. Ejima, J. J. Richardson, F. Caruso, *Nano Today* **2017**, *12*, 136 – 148; b) J. Guo, M. Suástegui, KK. Sakimoto, VM. Moody, G. Xiao, DG. Nocera, NS. Joshi, *Science.* **2018**, *362*, 813 – 816.
[9] W. Luo, G. Xiao, F. Tian, J. J. Richardson, Y. Wang, J. Zhou, J. Guo, X. Liao, B. Shi, *Energy Environ. Sci.* **2019**, *12*, 607 – 614.
[10] G. Frey, H. Peng, S. Rits-Volloch, M. Morelli, Y. Cheng, B. Chen, *Proc. Natl. Acad. Sci. USA* **2008**, *105*, 3739 – 3744.
[11] D. Bastian, H. Borel, T. Sasaki, A. D. Steinberg, Y. Borel, *J. Immunol.* **1985**, *135*, 1772 – 1777.
[12] Q. Fu, M. M. Shaik, Y. Cai, F. Ghantous, A. Piai, H. Peng, S. Rits-Volloch, Z. Liu, S. C. Harrison, M. S. Seaman, B. Chen, J. J. Chou, *Proc. Natl. Acad. Sci. USA* **2018**, *115*, E8892 – E8899.
[13] a) T. Muster, F. Steindl, M. Purtscher, A. Trkola, A. Klima, G. Himmler, F. Ruker, H. Katinger, *J. Virol.* **1993**, *67*, 6642 – 6647; b) G. Stiegler, R. Kunert, M. Purtscher, S. Wolbank, R. Voglauer, F. Steindl, H. Katinger, *AIDS Res. Hum. Retroviruses* **2001**, *17*, 1757 – 1765; c) J. Huang, G. Ofek, L. Laub, M. K. Louder, N. A. Doria-Rose, N. S. Longo, H. Imamichi, R. T. Bailer, B. Chakrabarti, S. K. Sharma, S. M. Alam, T. Wang, Y. Yang, B. Zhang, S. A. Migueles, R. Wyatt, B. F. Haynes, P. D. Kwong, J. R. Mascola, M. Connors, *Nature* **2012**, *491*, 406 – 412; d) L. D. Williams, G. Ofek, S. Schätzle, J. R. McDaniel, X. Lu, N. I. Nicely, L. Wu, C. S. Lougheed, T. Bradley, M. K. Louder, K. McKee, R. T. Bailer, S. O'Dell, I. S. Georgiev, M. S. Seaman, R. J. Parks, D. J. Marshall, K. Anasti, G. Yang, X. Nie, N. L. Tumba, K. Wiehe, K. Wagh, B. Korber, T. B. Kepler, S. M. Alam, L. Morris, G. Kamanga, M. S. Cohen, M. Bonsignori, S. M. Xia, D. C. Montefiori, G. Kelsoe, F. Gao, J. R. Mascola, M. A. Moody, K. O. Saunders, H. X. Liao, G. D. Tomaras, G. Georgiou, B. F. Haynes, *Sci. Immunology* **2017**, *2*, eaal2200.
[14] J. Dev, D. Park, Q. Fu, J. Chen, H. J. Ha, F. Ghantous, T. Herrmann, W. Chang, Z. Liu, G. Frey, M. S. Seaman, B. Chen, J. J. Chou, *Science* **2016**, *353*, 172 – 175.
[15] S. Lata, A. Reichel, R. Brock, R. Tampe, J. Piehler, *J. Am. Chem. Soc.* **2005**, *127*, 10205 – 10215.
[16] C. Tian, X. Li, Z. Liu, W. Jiang, G. Wang, C. Mao, *Angew. Chem. Int. Ed.* **2014**, *53*, 8041 – 8044; *Angew. Chem.* **2014**, *126*, 8179 – 8182.
[17] S. J. Flora, V. Pachauri, *Int. J. Environ. Res. Public Health* **2010**, *7*, 2745 – 2788.
[18] a) M. B. Zwick, *Aids* **2005**, *19*, 1725 – 1737; b) A. Hinz, G. Schoehn, H. Quendler, D. L. Hulsik, G. Stiegler, H. Katinger, M. S. Seaman, D. Montefiori, W. Weissenhorn, *Virology* **2009**, *390*, 221 – 227.
[19] J. Chen, G. Frey, H. Peng, S. Rits-Volloch, J. Garrity, M. S. Seaman, B. Chen, *J. Virol.* **2014**, *88*, 1249 – 1258.

Manuscript received: March 12, 2019
Accepted manuscript online: April 16, 2019
Version of record online: May 7, 2019

Supporting Information

Unidirectional presentation of membrane proteins in nanoparticle-supported liposomes

Wen Chen[+], Junling Guo[+], Yongfei Cai, Qingshan Fu, Bing Chen, James J. Chou*

Abstract: Presentation of membrane proteins to host immune systems has been a challenging problem due to complexity arising from the poor *in vivo* stability of the membrane-mimetic media often used for solubilizing the membrane proteins. We report the use of functionalized, biocompatible nanoparticles as substrates to guide the formation of proteoliposomes that can present many copies of membrane proteins in a unidirectional manner. The approach was demonstrated to present the membrane-proximal region of the HIV-1 envelope glycoprotein. These nanoparticle-supported liposomes are broadly applicable as membrane antigen vehicles for inducing host immune responses.

Table of Contents

Experimental Procedures

Gold-polyphenol nanoparticle production and functionalization. 0.8 mg/ml of tannic acid (Sigma Aldrich) was prepared in ddH_2O. Chloroauric acid (Sigma Aldrich) was added to tannic acid solution drop by drop to the final concentration of 0.4 mM. The mixture was incubated at room temperature with stirring at 800 rpm for 20 minutes to form polyphenol-stabilized gold nanoparticles (AuNPs). AuNPs were spun down at 12,000 g for 10 minutes. Pellet was then washed with ddH_2O. Resuspended AuNPs in ddH_2O was thoroughly sonicated before centrifugation again. The centrifugation and washing steps were repeated twice. AuNPs were then mixed with 0.04% glutaraldehyde (Electron Microscopy Sciences) and 0.5 mg/ml N_α,N_α-Bis(carboxymethyl)-L-lysine (Lysine-NTA) (Sigma Aldrich) at 45°C for 1 hour. The conjugated NTA-AuNPs were then spun down and washed with ddH_2O for three times. 0.5 mM $NiCl_2$ was added to the NTA-AuNP solution. Ni-NTA-AuNPs were then washed with ddH_2O for four times and stored at 4°C upon further use.

Zeta-potential measurement. The zeta-potentials were measured using a Zetasizer Nano-ZS (Malvern Instruments, UK) with a 633 nm He-Ne ion laser. The capsules were suspended in 10 mM phosphate buffer (pH 7.4) before adding different nanoparticle solutions. Measurements were repeated three times. The results were expressed as the mean and standard deviation obtained from the three measurements.

Interaction between Ni-NTA-AuNPs and His_6-tag. Foldon is the C-terminal domain of T4 fibritin containing 27 residues and forms highly-stable trimer[1]. Foldon with C-terminal His_6-tag was cloned into the pET-15 vector and expressed in BL21(DE3) cells at 37°C (induced with 1 mM isopropyl-β-d-thiogalactopyranoside (IPTG) for 6 hours). The protein was purified by Ni-NTA affininity (HisPur Ni-NTA resin, Thermo Fisher) and size exclusion chromatography (superdex 75 column, GE Healthcare). The NMR oneone echo experiment was used to record the 1D ^1H spectrum of a 450 µl Foldon sample (30 µM Foldon, 25 mM phosphate, 50 mM NaCl, pH 7.2) before and after mixing with 100 µl of Ni-NTA-AuNP solution (OD_{530}=0.1) in the same buffer. In the latter, the volume of the mixture was concentrated back to 450 µl before NMR measurement.

MPER-TMD plasmid construction. The MPER-TMD corresponds to a fragment of HIV-1 gp41 (clade D, isolate 92UG024.2) spanning residues 660-710; it contains the entire MPER (residues 660-683) and the TMD (residues 684-705). FLAG-tag and His_6-tag sequences were added to the N- and C-termini of the MPER-TMD, respectively. The FLAG-MPER-TMD-His_6 DNA was cloned into the pMM-LR6 vector as a fusion to the C-terminus of the trpLE sequence.

MPER-TMD expression and purification. The MPER-TMD plasmid was transformed into *E.coli* BL21(DE3) for expression. Cell cultures were grown at 37° C in LB media until OD_{600} reached 0.6, and cooled to 22° C before induction with 100 µM isopropyl β-D-thiogalatopyranoside (IPTG) at 22° C for overnight. The MPER-TMD was extracted from inclusion bodies, cleaved by cyanogen bromide, and purified by HPLC as described previously[2]. The purified MPER-TMD were lyophilized and validated by SDS-PAGE and MALDI-TOF mass spectrometry.

Reconstitution of MPER-TMD in bicelles. 2 mg of lyophilized MPER-TMD powder was mixed with 9 mg of 1,2-dimyristoyl-sn-Glycero-3-Phosphocholine (DMPC, Avanti Polar Lipids) in hexafluoro-isopropanol. The mixture was blown dry to a thin film in a glass vial under nitrogen gas, followed by overnight lyophilization. The dried thin film was dissolved in 3 ml of 8 M urea containing 20 mg of 1,2-dihexanoyl-sn-Glycero-3-Phosphocholine (DH_6PC, Avanti Polar Lipids) and 4 mg of 1,2-diheptanoyl-sn-Glycero-3-Phophocholine (DH_7PC, Avanti Polar Lipids). The mixture was dialyzed twice against phosphate buffer (pH 7.2, 50 mM NaCl) (1 L each time) to remove urea. Additional DH_6PC was added to the sample every hour to compensate its loss due to dialysis. The DMPC:DH_6PC ratio was controlled between 0.5 and 0.6 by 1D NMR. Bicelle reconstituted MPER-TMD was concentrated to ~ 1 ml (around 0.3 mM) after dialysis.

Ni-NTA-AuNP supported proteoliposome formation. The Ni-NTA-AuNP solution (OD_{530}=0.1) and the bicelles-reconstituted MPER-TMD solution (~ 0.3 mM) were mixed at the ratio of 3:1 (vol/vol). The mixture was diluted 20 times by adding phosphate buffer (pH 7.2, 50 mM NaCl) before dialyzed against the same phosphate buffer to remove DH_6PC detergent. 10 kDa cut off dialysis cassette was used (Life technology). Buffer was changed every 3 hours for at least 6 times at 4°C.

Imaging interaction between antibody and MPER-TMD proteoliposome. Anti-FLAG or anti-His_6 antibody (Sigma) was added to Ni-NTA-AuNP-supported proteoliposome containing the FLAG-MPER-TMD-His_6. The amount of antibody was added at 1:1 molar ratio of antibody:MPER-TMD. The concentration of the MPER-TMD was estimated based on the assumption that all applied MPER-TMD (with known amount) were incorporated into the AuNP-supported proteoliposome. Antibodies and nanoparticle were mixed for 10 minutes at room temperature before analysis by negative staining EM.

DNA buckyball formation. DNA sequences for buckyball assemble were adapted from previous work[3]; long strand (L):aggcaccatcgtaggtttcttgccaggcaccatcgtaggtttcttgccagg-caccatcgtaggtttcttgcc; medium stand (M): tagcaacctgcctggcaagcctacgatggacacggtaacgcc; short strand (S): ttaccgtgtggttgctaggcg. Thiol modifier C6 S-S was added to the 3' of the long strand. TriNTA with a free primary amine (Fig. S4a) was synthesized by Medicilon Inc. (Shanghai, China) and stored as dry powder at

-20°C. The bi-functional crosslinker PEG2-SMCC (succinimidyl 4-(N-maleimidomethyl)cyclohexane-1-carboxylate) was incubated with TriNTA (with 4:1 molar ratio) in 100 mM sodium carbonate buffer (pH 8.0) for 1 hour, which achieved > 95% reaction efficiency. The SMCC-linked TriNTA was then purified by RP-HPLC using a Zorbax SB-C18 semi-preparative column (Agilent) and a gradient of 5-20% acetonitrile in 0.1 M Triethylammonium Acetate (TEAA) (Calbiochem). SMCC-TriNTA was lyophilized and stored at -80°C upon further use.

To functionalize the L DNA strand with TriNTA, 100 μM of thiol-modified L strand was dissolved in 25 mM HEPES buffer (pH 7.4), and reduced by 20 mM DTT for 10 minutes. The DTT-treated L solution was applied to PD-10 column (GE Healthcare) to remove DTT, followed by immediate mixing with 2 times excess amount of SMCC-TriNTA in HEPES buffer (pH 7.4). The reaction mixture was degassed for 30 min and incubated for additional 30 min at room temperature. Ni^{2+} was added to TriNTA-L conjugate at 3:1 molar ratio. The Ni-TriNTA-L conjugate was purified using a His_6-tag column, made in the lab by chemically linking the Foldon-His_6-tag to NHS-activated agrose resin (Thermo Fisher Scientific). The Ni-TriNTA-L conjugate was mixed with the Foldon-His_6-tag resin for 30 minutes, and eluted with 200 mM imidazole (Fig. S4b). Pure Ni-TriNTA-L conjugate was stored in TA/Mg^{2+} buffer (40 mM Tris, 20 mM acetic acid, 12.5 mM magnesium acetate, pH 8.0) after removing imidazole.

Finally, the Ni-TriNTA-L, the M, and the S were mixed at molar ratio of 1:3:3 in TA/Mg^{2+} buffer. The final concentration of TriNTA-L was adjusted to 70 nM. The DNA buckyball assembly was achieved using two steps of annealing: 1) from 95°C to 65°C, at a rate of 1 degree per 15 min; 2) from 65°C to 20˚C, at a rate of 1 degree per hour. DNA buckyball assembly was accessed by electrophoresis using 0.5% agarose gel (Fig. S5a). The DNA buckyball solution was concentrated ([TriNTA-L] ≥ 400 nM) before examined by negative staining EM.

DNA Buckyball supported proteoliposome formation. Bicelle-reconstituted MPER-TMD (with C-terminal His_6-tag) was mixed with the TriNTA functionalized DNA buckyball at the molar ratio of 1 trimeric MPER-TMD to 1 TriNTA-L strand. The mixture was passed through PD-10 column twice to remove DH_6PC detergent. The elution from PD-10 was concentrated ([TriNTA-L] ≥ 400 nM) before analysis by negative staining EM.

Electron Microscopy sample preparation. To examine AuNP alone by EM, 2.5 ul of AuNP solution (OD_{530}=0.1) was loaded onto nickel grid with formvar/carbon film (Electron Microscopy Sciences), and dried in air for at least 2 hours. For DNA buckyball and all nanoparticle-supported liposomes, samples were loaded onto copper grid with formvar/carbon film (Electron Microscopy Sciences). The Ni-NTA-AuNP-supported MPER-TMD proteoliposomes were negatively stained by 1.5% Uranyl formate. DNA buckyball and DNA buckyball-supported MPER-TMD proteoliposomes were first concentrated ([TriNTA-L] ≥ 400 nM), and then negatively stained by 1.5% Uranyl formate. EM images were taken using the CM10 electron microscope (Philips).

Results and Discussion

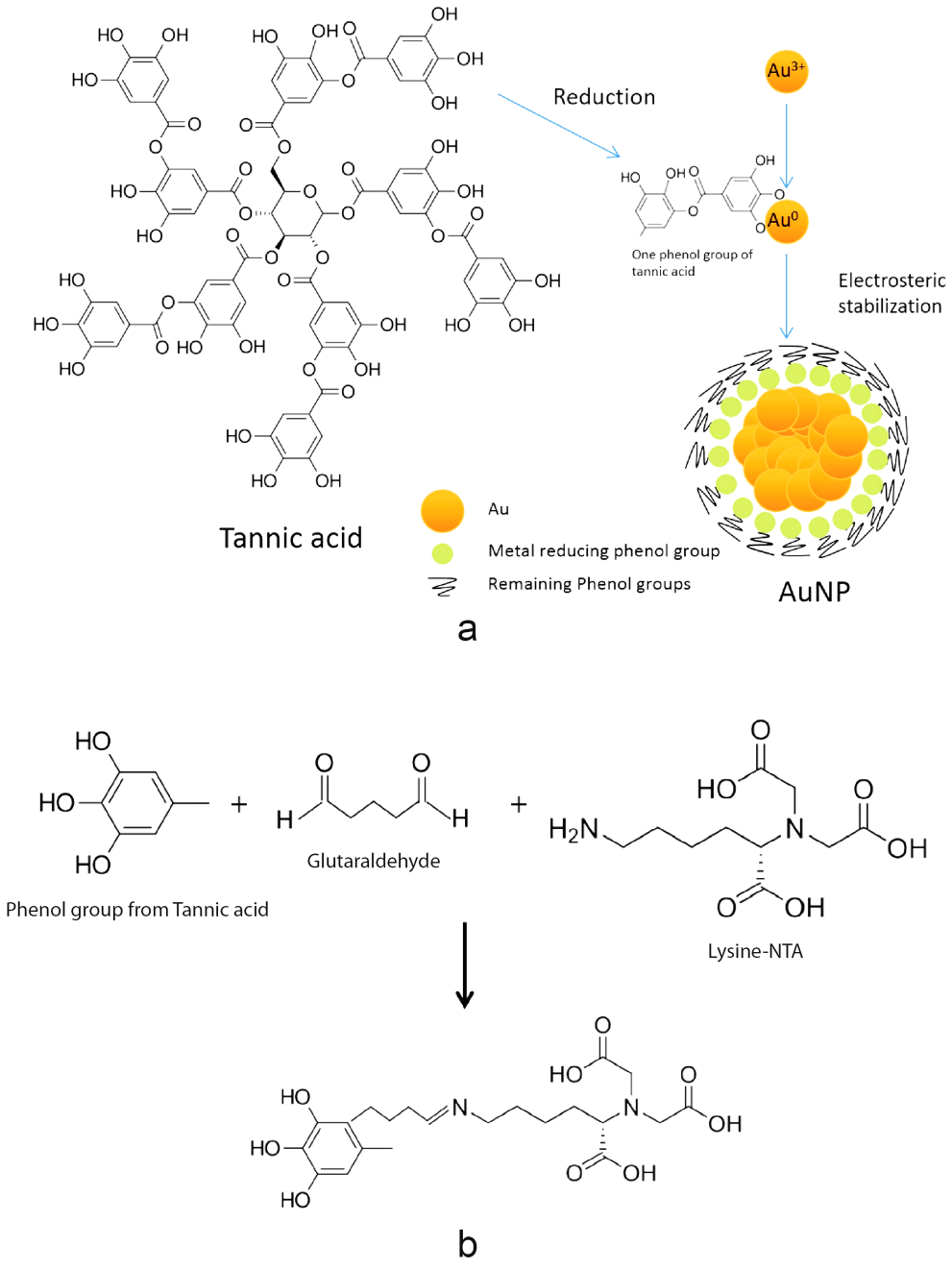

Figure S1. Schematic illustration of AuNP synthesis and functionalization

(a) Reaction mechanism of gold nanoparticle synthesis and stabilization by tannic acid. Phenolic hydroxyl group (-OH) of tannic acid can reduce the gold precursor and coordinate with gold. The rest of polyphenol groups can act as surfactant to stabilize the gold ion with electrostatic interaction.

(b) Glutaraldehyde is used to conjugate primary amine of lysine-NTA and nucleophilic carbons from tannic acid's phenol group.

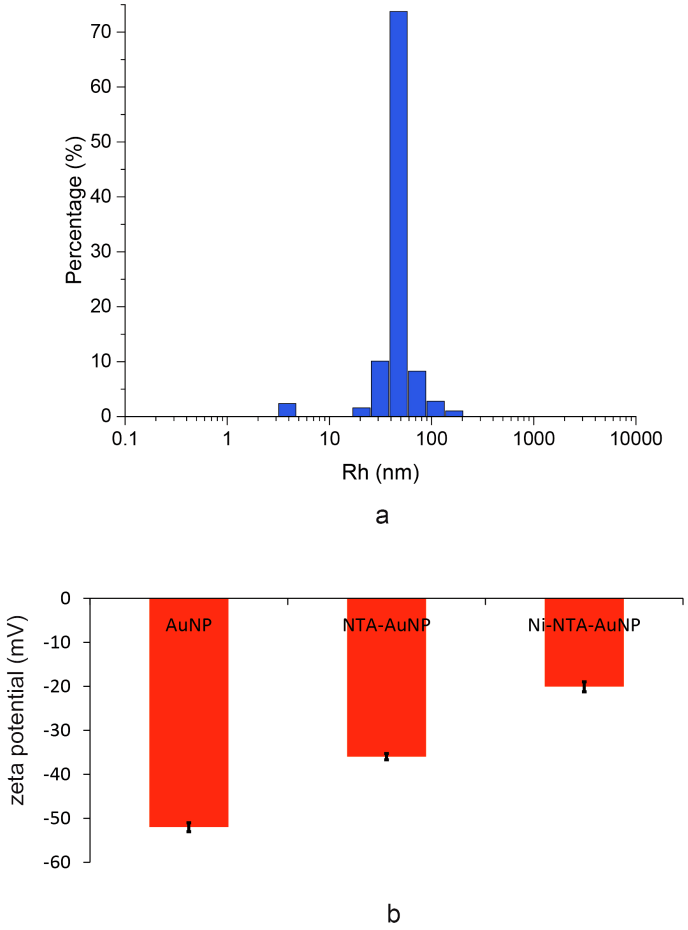

Figure S2. Characterization of polyphenol-stabilized gold nanoparticles

(a) Dynamic light scattering (DLS) of polyphenol-stabilized AuNPs. DLS result shows that AuNPs are very homogenous, with diameter around 47 nm.

(b) Surface charges of AuNPs, NTA-AuNPs, and Ni-NTA-AuNPs were measured by Zetasizer Nano-ZS equipment. The zeta potentials (ζ) of AuNPs, NTA-AuNPS, and Ni-NTA-AuNPs are -51 mV, -36 mV, and -20.1 mV, respectively. The values are vastly different due to different surface properties of nanoparticles, indicating the successful functionalization of AuNPs at each stage.

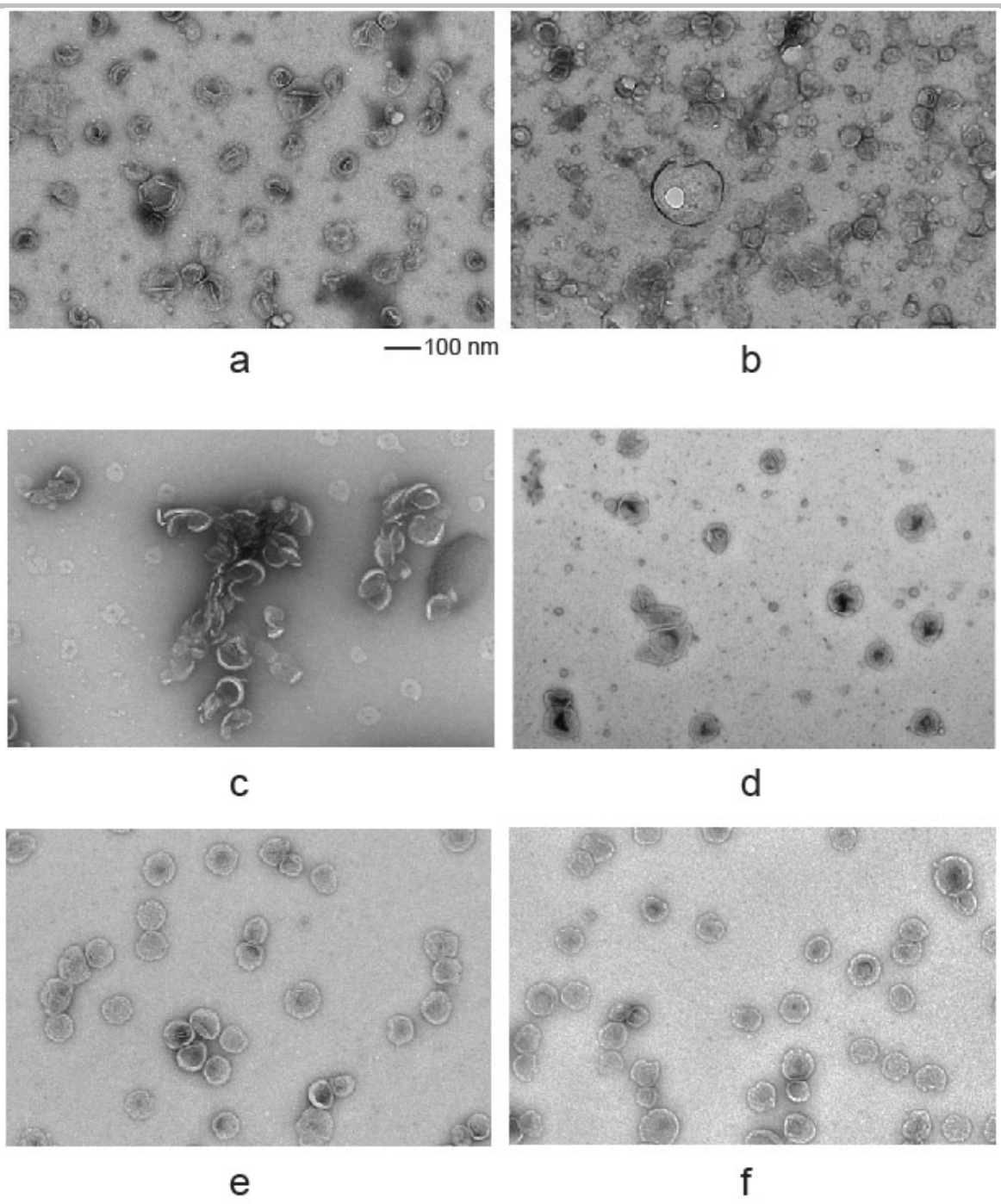

Figure S3. Controls for nanoparticle-supported liposome formation examined by negative stain EM

(a) Liposome formation from empty bicelles without Ni-NTA-AuNPs. 5 µl of bicelle buffer (45 mM DH_6PC, 20 mM DMPC) was diluted by adding 400 µl of 25 mM phosphate buffer (pH 7.2). After DH_6PC was removed through dialysis, 3.5 µl of sample was loaded onto copper grid.

(b) Liposome formation from empty bicelles with Ni-NTA-AuNPs. 15 µl of Ni-NTA-AuNPs (OD_{530} = 0.1) was mixed with 5 µl of bicelle buffer (45 mM DH_6PC, 20 mM DMPC). The mixture was diluted 20x by adding 400 µl of 25 mM phosphate buffer (pH 7.2). After DH_6PC was removed, 3.5 µl of sample was loaded onto copper grid.

(c) Liposome formation from bicelle-reconstituted MPER-TMD-His_6 with non-functionalized AuNPs. 15 µl of non-functionalized AuNP solution (OD_{530} = 0.1) was mixed with 5 µl of MPER-TMD sample (0.3 mM MPER-TMD, 45 mM DH_6PC, 20 mM DMPC). The same dilution and dialysis steps were used before examined by negative staining EM.

(d) Liposome formation from bicelle-reconstituted MPER-TMD-His_6 with Ni-NTA-functionalized AuNPs. The volume ratio between Ni-NTA-AuNP solution (OD_{530} = 0.1) and the MPER-TMD sample (0.3 mM, 45 mM DH_6PC, 20 mM DMPC) is set at 1:1. Detailed liposome formation and negative staining EM procedures are described in methods.

(e) Liposome formation from bicelle-reconstituted MPER-TMD-His_6 with Ni-NTA-functionalized AuNPs. The volume ratio between Ni-NTA-AuNP solution (OD_{530} = 0.1) and the MPER-TMD sample (0.3 mM, 45 mM DH_6PC, 20 mM DMPC) is set at 3:1.

(f) Liposome formation from bicelle-reconstituted MPER-TMD-His_6 with Ni-NTA-functionalized AuNPs. The volume ratio between Ni-NTA-AuNP solution (OD_{530} = 0.1) and the MPER-TMD sample (0.3 mM, 45 mM DH_6PC, 20 mM DMPC) is set at 6:1.

Note: Naked AuNPs and Ni-NTA-AuNPs could not be observed due to incompatibility with negative staining.

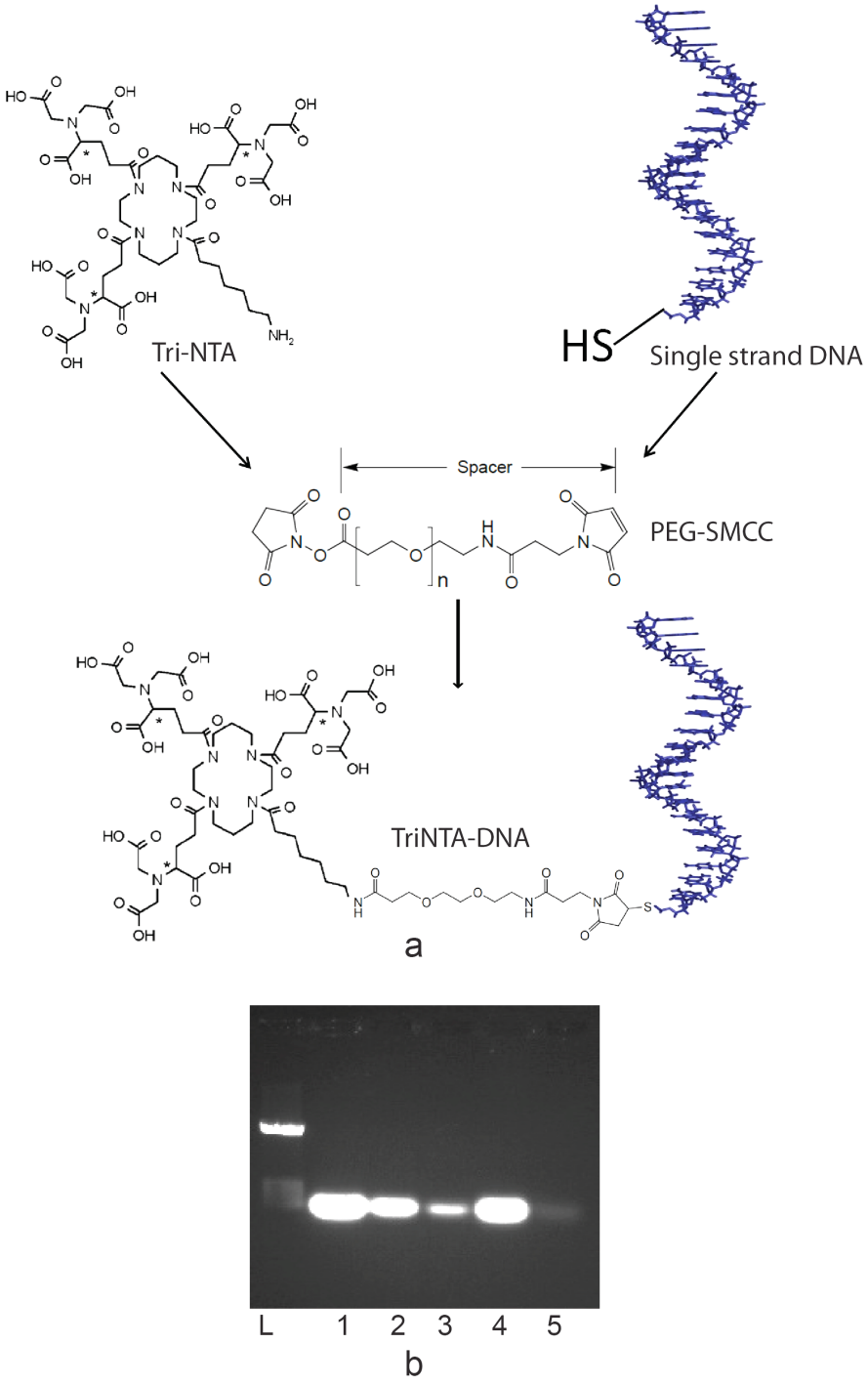

Figure S4. Preparation of TriNTA-functionalized single stranded DNA

(a) The reaction scheme used to conjugate the primary amine of TriNTA to the thiol group of synthesized DNA via bi-functional PEG2-SMCC linker. In the scheme, the NHS ester of SMCC reacts with the amine group of TriNTA with extremely high efficiency (>95%). The SMCC maleimide group reacts with the thiol group of DNA.

(b) TriNTA-functionalized DNA purification steps analyzed by agarose gel. The TriNTA-PEG2-SMCC, purified by HPLC, was mixed with the thiol-modified L strand to form TriNTA-L conjugate. After the reaction, the TriNTA-L was charged with Ni^{2+}. Detailed procedure can be found in methods section. The gel lanes are: L – DNA ladder; 1 – TriNTA-L reaction mixture; 2 – flow-through of the reacted solution from Foldon-His_6-tag resin; 3 – wash of the resin to remove unbound species; 4 – elution from the resin with 0.2 M imidazole; 5 – further elution with 0.5 M imidazole.

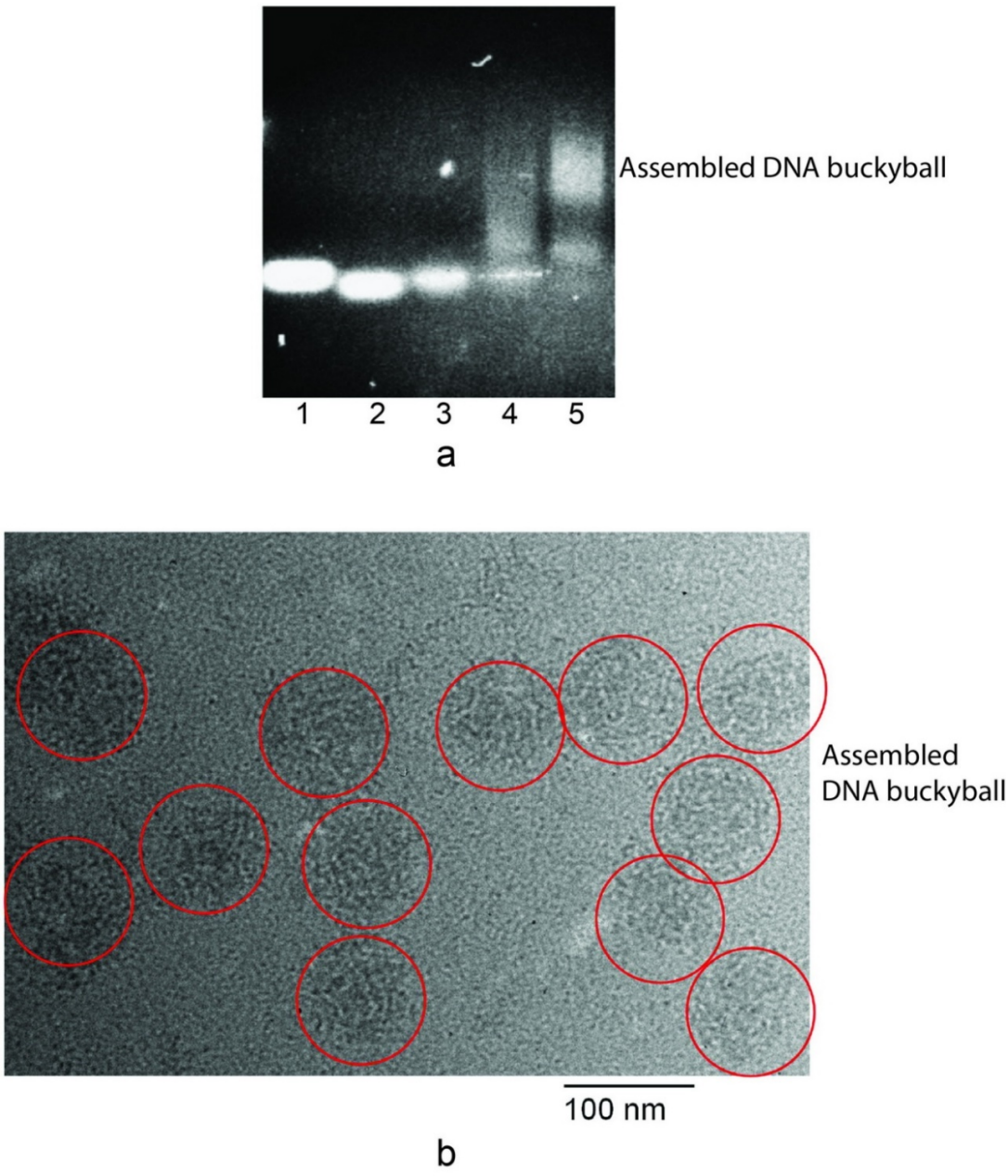

Figure S5. DNA buckyball formation

(a) Agarose gel analysis of DNA buckyball formation using the TriNTA-functionalized L strand and regular M and S strands. Lane 1: pure Ni-TriNTA-L strand; Lane 2: pure M strand; Lane 3: pure S strand; Lane 4: after direct mixing of Ni-TriNTA-L, M, and S, at 1:3:3 molar ratio; Lane 5: after two-step annealing treatment of the mixed sample (details in Methods). Comparison of the higher and lower bands suggests that the efficiency of DNA buckyball formation is ~90%.
(b) The assembled DNA buckyball sample was negatively stained and observed using the CM10 electron microscope. The EM image shows mostly homogenous assemblies with diameter ~ 80 nm.

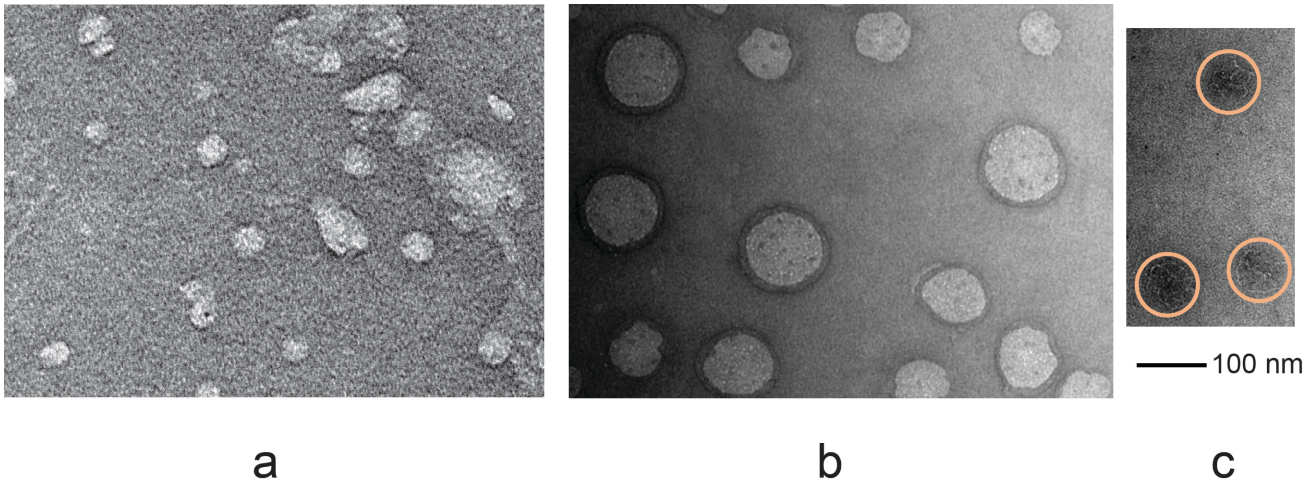

Figure S6. Proteoliposome formation guided by functionalized DNA buckyballs

(a) Negative stain EM image of liposomes formed by mixing functionalized DNA buckyballs and empty bicelles, showing highly inhomogeneous liposomes. 143 µl of DNA buckyball ([Tri-NTA-L] = 70 nM) was mixed with 1 µl of bicelle buffer (45 mM DH_6PC, 20 mM DMPC). The mixture was treated with PD-10 column twice, then examined by negative staining EM. Detailed procedures are described in methods.

(b) Negative stain EM image of liposomes formed by mixing functionalized DNA buckyballs and bicelle-reconstituted MPER-TMD-His_6, showing much better defined shape and size. 143 µl of DNA buckyball ([Tri-NTA-L] = 70 nM) was mixed with 1 µl of MPER-TMD-His_6 (0.3 mM MPER-TMD, 45 mM DH_6PC, 20 mM DMPC). **Note**: some incompletely assembled buckyballs could also support liposome assembly, resulting in smaller liposomes.

(c) Negative stain EM image of the naked DNA buckyball, showing that the size is consistent with those observed in (b).

Author Contributions

W.C., J.G., B.C., and J.J.C. conceived the study; J.G. and W.C. prepared functionalized nanoparticles; Y.C., Q.F., W.C. prepared membrane protein samples; J.J.C. and W.C. wrote the paper and all authors contributed to the editing of the paper.

References

[1] T. Abe, T. Oka, A. Nakagome, Y. Tsukada, T. Yasunaga, M. Yohda, *J Biochem* **2011**, *150*, 403-409.

[2] a) Q. Fu, M. M. Shaik, Y. Cai, F. Ghantous, A. Piai, H. Peng, S. Rits-Volloch, Z. Liu, S. C. Harrison, M. S. Seaman, B. Chen, J. J. Chou, *Proceedings of the National Academy of Sciences of the United States of America* **2018**, *115*, E8892-E8899; b) J. Dev, D. Park, Q. Fu, J. Chen, H. J. Ha, F. Ghantous, T. Herrmann, W. Chang, Z. Liu, G. Frey, M. S. Seaman, B. Chen, J. J. Chou, *Science* **2016**, *353*, 172-175.

[3] Y. He, T. Ye, M. Su, C. Zhang, A. E. Ribbe, W. Jiang, C. Mao, *Nature* **2008**, *452*, 198-201.